The impact of tumor receptor heterogeneity on the response to anti-angiogenic cancer treatment

Ding Li[a] and Stacey D. Finley[a,b]*

[a] Department of Biomedical Engineering, University of Southern California, Los Angeles, California, United States of America

[b] Department of Chemical Engineering and Materials Science, University of Southern California, Los Angeles, California, United States of America

* Corresponding author

Running title. Receptor heterogeneity affects anti-angiogenic treatment

Keywords: systems biology; pharmacokinetic/pharmacodynamic model; anti-VEGF; TSP1 mimetic; mathematical modeling

Financial support. The authors acknowledge the support of the US National Science Foundation (CAREER Award 1552065 to S.D.F.) and the American Cancer Society (130432-RSG-17-133-01-CSM to S.D.F.). The funders had no role in study design, data collection and analysis, decision to publish, or preparation of the manuscript.

Corresponding author information.

Stacey D. Finley
1042 Downey Way, DRB 140
Los Angeles, CA 90089
Phone: 213-740-8788; Fax: 213-821-3897
Email: sfinley@usc.edu

Abstract

Multiple promoters and inhibitors mediate angiogenesis, the formation of new blood vessels, and these factors represent potential targets for impeding vessel growth in tumors. Vascular endothelial growth factor (VEGF) is a potent angiogenic factor targeted in anti-angiogenic cancer therapies. In addition, thrombospondin-1 (TSP1) is a major endogenous inhibitor of angiogenesis, and TSP1 mimetics are being developed as an alternative type of anti-angiogenic agent. The combination of bevacizumab, an anti-VEGF agent, and ABT-510, a TSP1 mimetic, has been tested in clinical trials to treat advanced solid tumors. However, the patients' responses are highly variable and show disappointing outcomes. To obtain mechanistic insight into the effects of this combination anti-angiogenic therapy, we have constructed a novel whole-body pharmacokinetic model including the VEGF and TSP1 reaction networks. Using this molecular-detailed model, we investigated how the combination anti-angiogenic therapy changes the extracellular angiogenic balance in cancer patients and how the effect of the combination therapy is influenced by tumor receptor expression. Overall, this model complements the clinical administration of combination anti-angiogenic therapy, highlights the role of tumor receptor variability in the heterogeneous responses to anti-angiogenic therapy and identifies the tumor receptor profiles that correlate with a high likelihood of a positive response to combination therapy. In addition, this study provides novel understanding of the VEGF-TSP1 balance in cancer patients at the systems-level and could be further used to optimize combination anti-angiogenic therapy.

Major Findings

To help the design and analysis of anti-angiogenic tumor therapy, we constructed the first computational framework that enables the study of the combination anti-angiogenic therapy targeting both VEGF and TSP1 signaling. The model illustrates how the combination of bevacizumab and ABT-510 modulates the angiogenic balance of VEGF and TSP1 in the body and predicts the impact of tumor receptor heterogeneity on the response to this combination therapy. The levels of VEGF receptor R1 and TSP1 receptors CD36 and CD47 on tumor cells were identified as potential tissue biomarkers predicting the response to combination therapy. The predictions of this model have important clinical relevance – to recapitulate and explain several results reported in clinical trials of anti-angiogenic therapy.

Quick Guide to Equations and Assumptions

The mechanistic model represents human cancer patients using three compartments: normal tissue ("normal," represented by skeletal muscle), the vasculature ("blood"), and diseased tissue ("tumor") (***Fig. 1A***). The soluble species are assumed to diffuse within the available interstitial space very fast compared to the timescale of the biochemical reactions[1], thus the compartment is well-mixed with uniform distribution of molecules within the compartment volume. The characterization of the species dynamics is based on the principles of mass action kinetics and biological transport. Given the complexity of the system, a rule-based modeling approach is used to construct the model[2]. The biological reaction rules are defined in BioNetGen, which automatically generates the model of ordinary differential equations (ODEs). The defined rules generate 561 species and 2618 reactions. We implemented and solved the ODEs in MATLAB (model file provided in ***Supplementary File S1***). Here, we list several generic forms of equations as an overview of ODE model.

i. Key equations

$$\frac{d[L]_C}{dt} = q_L^C + k_{cat,PreL}[PreL]_C - k_{deg}[L]_C - k_{cat,L}[L]_C - \left(\frac{k_{lym} + k_{pL}^{CB} S_{CB}}{U_C}\right)\frac{[L]_C}{K_{AV,C}} + k_{pL}^{CB}\frac{S_{CB}}{U_C}\frac{U_B}{U_p}[L]_B + \sum\left(k_{off,L,R_i}[LR_i]_C - k_{on,L,R_i}[L]_C[R_i]_C\right)$$

This equation describes the change over time of the concentration of a generic soluble species $[L]_C$ in the interstitial space of compartment *C* (tumor or normal tissue). q_L^C represents the overall secretion of species L in compartment *C*. This secretion rate is the sum of the secretion from abluminal endothelial and parenchymal cells. The second term represents the generation from a precursor $[PreL]_C$ with catalytic rate $k_{cat,PreL}$. $k_{deg}[L]_C$ and $k_{cat,L}[L]_C$ characterize the degradation and the enzyme catalyzed conversion, respectively. The inter-compartmental transport from tumor or normal tissue to blood is mediated by lymphatics, with a rate constant of k_{lym}, and microvascular permeability, with rate constant k_{pL}^{CB}. S_{CB} is the total surface of microvessels at the tissue-blood interface. U_C is the total volume of tissue *C*. $K_{AV,C}$ represents the available volume fraction for soluble ligands in tissue *C*. The term $\frac{U_B}{U_p}$ is the available fluid volume fraction for ligand in the blood, with U_B and U_p indicating the blood and plasma volumes, respectively. The last term represents the summation of all rates in which the species binds to an individual receptor, coupled receptor, other soluble species or the binding sites in extracellular matrix and basement membranes.

Similarly, for a soluble species in blood, the ODE can be generalized as in the following example. c_L is the clearance rate in blood. The transportation is comprised of contributions between tumor and blood (*TB*) and normal and blood (*NB*).

$$\frac{d[L]_B}{dt} = q_L^B + k_{cat,PreL}[PreL]_B - c_L[L]_B - k_{cat,L}[L]_B + \left(\frac{k_{lym} + k_{pL}^{NB} S_{NB}}{U_B}\right)\frac{[L]_N}{K_{AV,N}} - k_{pL}^{NB}\frac{S_{NB}}{U_p}[L]_B + \frac{k_{pL}^{TB} S_{TB}}{U_B}\frac{[L]_T}{K_{AV,T}} - k_{pL}^{TB}\frac{S_{TB}}{U_p}[L]_B + \sum\left(k_{off,L,R_i}[LR_i]_B - k_{on,L,R_i}[L]_B[R_i]_B\right)$$

The receptors dynamic can be generalized as follows. Receptors are localized on the cell surfaces and are not transported between compartments. *C* denotes the compartment (*T*: tumor, *N*: normal, or *B*: blood). *P* denotes the cell type: tumor parenchymal cells, tumor endothelial cells, normal endothelial cells or normal tissue parenchymal cells. Receptors are assumed to be internalized at a rate of $k_{int,R}$ and can be recycled to cell surface with rate $S_{R,C}$. They bind and unbind to ligands (with rate constants $k_{on,L_i,R}$ and $k_{off,L_i,R}$) or couple with and dissociate from co-receptors (with rate constants $k_{c,R_i,R}$ and $k_{dissoc,R_i,R}$).

$$\frac{d[R]_{C,P}}{dt} = S_{R,C} - k_{int,R}[R]_{C,P} + \sum\left(k_{on,L_i,R}[L_i]_C[R]_{C,P} + k_{off,L_i,R}[L_iR]_C\right) + \sum\left(k_{c,R_i,R}[R_i]_{C,P}[R]_{C,P} + k_{dissoc,R_i,R}[R_iR]_{C,P}\right)$$

The intravenous infusion of bevacizumab is modeled as introducing secretion of bevcizumab in blood for a time interval $\Delta t_{infusion}$. The subcutaneous bolus injection of ABT-510 is modeled as changing the concentration of ABT-510 in the subcutaneous compartment. Simulating the clinical protocol, bevacizumab is given every two weeks and ABT-510 is given twice daily. We define the angiogenic balance as the ratio of the concentrations of the pro-angiogenic complexes to the anti-angiogenic complexes. Specifically, the pro-angiogenic complexes include the ligand-bound VEGF receptors that are not interacting with active TSP1 receptors. Here we assume ligand bound VEGF receptor coupled with active TSP1 receptor is not a pro-angiogenic complex, since the downstream signaling of the ligand-bound VEGF receptor could be inhibited by TSP1[3,4]. The anti-angiogenic complexes are the active TSP1 receptors, those bound to TSP1 or the TSP1 mimetic. The fold-change of angiogenic ratio in tumor compartment (*F*) characterizes the response to anti-angiogenic treatment. $[VEGF{:}Rec]$ is the total concentration of pro-angiogenic complexes. $[TSP1{:}Rec]$ is the total concentration of anti-angiogenic complexes. *T* denotes Tumor compartment, and *t* indicates the simulated time: before treatment (*t* = 0 day) and after one cycle of treatment (*t* = 14 days).

$$F = \frac{Angiogenic\ Ratio\ (Post{-}treatment)}{Angiogenic\ Ratio\ (Pre{-}treatment)} = \frac{\frac{[VEGF{:}Rec]_T^{t=14}}{[TSP1{:}Rec]_T^{t=14}}}{\frac{[VEGF{:}Rec]_T^{t=0}}{[TSP1{:}Rec]_T^{t=0}}}$$

ii. Major assumptions

Our model is a significant extension of previous models. Several new soluble species are introduced into the model for the TSP1 reaction network. We assume that the newly introduced species have the same transport rates as the VEGF. In the model, the luminal endothelium is distinct from abluminal endothelium, and we assume the receptors are equally distributed on the two sides of endothelial cells. The pharmacokinetic data of bevacizumab and ABT-510 during combination therapy is not available. Therefore, we assume their pharmacokinetics are not influenced by one other during the combination therapy and are the same as what has been measured in clinical trials using them as single agents. To match the pharmacokinetic data of ABT-510, we assume the drug has a bioavailability of 30%.

1. Introduction:

Angiogenesis is a hallmark of cancer that facilitates tumor progression in many aspects[5]. Tumor growth relies on the formation of new blood vessels to enable waste exchange and to deliver oxygen and nutrients to the tumor. In addition, angiogenesis increases the likelihood of metastasis by enabling tumor cells to enter the bloodstream and disperse to other sites in the body[6]. Considering the outstanding importance of angiogenesis for tumor development, anti-angiogenic therapy was designed to starve the tumor of its nutrient supply and limit its growth[7].

Tumor angiogenesis is controlled by both pro-angiogenic and anti-angiogenic signaling[8–10]. Common anti-angiogenic therapy uses single agents to reduce the pro-angiogenic signals. The primary anti-angiogenic agents being used in the clinic inhibit signaling mediated by the vascular endothelial growth factor-A (VEGF), a potent promoter of angiogenesis. However, this approach is not effective in all cancers. For example, bevacizumab, a monoclonal antibody that binds VEGF, is no longer approved for breast cancer treatment, and sunitinib, a tyrosine kinase inhibitor that targets VEGF receptors and other growth factor receptors, has also shown limited success[11]. These limitations of anti-VEGF treatment prompt the need for alternative approaches to target the tumor vasculature. One alternate anti-angiogenic approach is to enhance the signal of anti-angiogenic factors. Thrombospondin-1 (TSP1) is one of the most studied endogenous inhibitors of angiogenesis and has been shown to inhibit vascular growth and tumorigenesis in preclinical trials[12–14]. Inspired by the effect of TSP1, TSP1 mimetics were developed for tumor treatment[15]. One such drug, named as ABT-510, reached Phase II clinical trials. However, ABT-510 failed to show clear evidence of efficacy and is no longer tested as a single-agent drug in clinical development[16,17].

The disappointing outcomes of clinical studies of anti-angiogenic drugs as single agents prompt the study of combination anti-angiogenic therapy. Administering a combination of anti-angiogenic agents that simultaneously target multiple angiogenic signals is expected to achieve efficient and durable suppression of angiogenesis by strong shifting the relative balance of inducers and inhibitors of angiogenesis to oppose the “angiogenic switch”[18,19]. The combination of agents targeting different pathways might also prevent tumors from leveraging complementary pathways to escape anti-angiogenic treatment. With this in mind, the TSP1 mimetic was clinically tested in combination with bevacizumab in patients with advanced solid tumors. However, patients displayed a heterogeneous response to this combination therapy[20]: one patient had a partial response and only 32% of the patients had prolonged stable disease (≥

6 months). Unfortunately, the mechanisms driving these disappointing results were not elucidated in the trial. Three fundamental questions remain: do the levels of TSP1 and VEGF balance one another in tumor tissue, how does combination therapy influence this VEGF-TSP1 balance, and does inter-patient heterogeneity lead to significantly different responses. Answering these questions contributes to our understanding of the action of combination therapy. In addition, considering the angiogenic balance at the levels of tissue, organs and the whole body can help us optimize anti-angiogenic therapy. In this study, we address these questions using a computational systems biology model.

Mathematical models provide a useful framework to study the response to anti-angiogenic treatment, complementing experimental and clinical studies. In particular, the effects of anti-VEGF agents on VEGF and its receptors have been intensively investigated using computational modeling[21]. A model of the VEGF-receptor system was previously used to illustrate the counterintuitive increasing of VEGF after anti-VEGF treatment[22], and our recent model of TSP1 and VEGF interactions in tumor tissue predicts the effects of various strategies mimicking TSP1's anti-angiogenic properties[23].

Here, we significantly expand on previous work to generate a novel whole-body model of the VEGF-TSP1 interaction network. We apply the model to understand how the angiogenic balance of VEGF and TSP1 is modulated by bevacizumab and ABT-510 combination therapy. We also use the model to investigate the impact of tumor receptor heterogeneity, which has been observed experimentally[24–27], on the response to combination anti-angiogenic therapy. The model predicts the receptors that can serve as predictive tissue biomarkers to distinguish the patients in which the combination anti-angiogenic therapy will elicit a strong therapeutic response. Overall, we establish a robust computational framework to predict the effects of anti-angiogenic therapies and understand clinical observations.

2. Materials and Methods

2.1 Rule Based Model of VEGF-TSP1 Reaction Network

The derivation of the ODE model is described in the Quick Guide to Equations and Assumptions. Here, we briefly summarize the defined rules that govern the molecular interactions and corresponding reactions (***Fig. 1B-G***). Following our previous works, the model includes two active VEGF isoforms ($VEGF_{165}$ and $VEGF_{121}$). The inactive form, $VEGF_{114}$, is the product of proteolytic cleavage of $VEGF_{165}$. Two predominant VEGF receptors, VEGFR1 and VEGFR2 (R1

and R2), and neuropilin co-receptors, NRP1 and NRP2 (N1 and N2), are considered (***Fig. 1B***). TSP1 binds to its receptors, CD36, CD47, low density lipoprotein receptor-related protein 1 (LRP1) and $\alpha_x\beta_1$ intergrins (β1, a generic form representing several species) (***Fig. 1C***). We also include matrix metalloproteinase, MMP, species (MMP3, MMP9 and proMMP9), which promote VEGF cleavage. TSP1 impedes the activation of MMP9 (***Fig. 1D***). Glycosaminoglycan (GAG) chains reside in the interstitial space, representing the extracellular matrix, as well as in the cellular basement membranes. GAG chains are able to bind and sequester TSP1 and $VEGF_{165}$ (***Fig. 1E***). The α-2-macroglobulin (α2M) species, a protease inhibitor, is confined to the blood compartment, where it binds to VEGF (***Fig. 1F***). The soluble species are introduced to the system by being secreted by cells and are removed from the system through degradation and clearance from the blood. Receptors are uniformly distributed on the cell surfaces and can be internalized by the cell and recycled back to the surface. The total number for each type of receptor is assumed to be conserved at every simulated time point. Transport of soluble species between the compartments is mediated by transcapillary permeability and lymphatic flow.

2.2 Model Parameters

All model parameters are described in the ***Supplementary File S2***, including the values extracted from literature where available. Secretion rates for the soluble species are tuned to match experimental measurements[28–33] (***Table 1***). Our steady state predictions of the species' concentrations quantitatively agree with the experimental data.

To investigate the impact of tumor receptor heterogeneity, we vary the receptor expression parameter values in the tumor compartment. In total, the densities of 16 receptors are varied in the simulations: four VEGF receptors on tumor cells (R1_Tum, R2_Tum, N1_Tum, N2_Tum), four TSP1 receptors on tumor cells (CD36_Tum, CD47_Tum, LRP1_Tum, β1_Tum), four VEGF receptors on tumor endothelial cells (R1_disEC, R2_disEC, N1_disEC, N2_disEC), and four TSP1 receptors on tumor endothelial cells (CD36_disEC, CD47_disEC, LRP1_disEC, β1_disEC). The densities of these receptors were randomly chosen from a uniform distribution within a range of 10-fold above and below the baseline value. We generated 1,000 different combinations of receptor density profiles, representing 1,000 unique cancer patients. We ran the model for each of the receptor profiles with anti-angiogenic treatment to examine how the response to treatment varies across the 1,000 parameter sets.

2.3 Combination Therapy of Bevacizumab and ABT-510

The combination therapy of bevacizumab and ABT-510 is simulated by mimicking the administration strategy used in clinical trials[20]. We first allowed the model to reach steady state (this occurs within 24 hours) before the start of treatment. We then simulated one cycle of the combination therapy: bevacizumab was administered once at the beginning of the cycle; ABT-510 was administered every 12 hours for 14 days. Bevacizumab was given at a dose of 10 mg/kg through intravenous infusion lasting 90 minutes, while ABT-510 was administered at 100 mg twice daily through subcutaneous injection. The kinetic parameters of bevacizumab are the same as those used in our previous work[28], which can capture the clinically-measured pharmacokinetic data[34] (***Supplementary Fig. S1A***). The bolus of ABT-510 was given directly to a subcutaneous compartment[35] (assumed to be a reservoir with a volume of 30 cm^3), and it is subsequently transported into blood. To fit the pharmacokinetic data of TSP1[36] (***Supplementary Fig. S1B***), we assumed the bioavailability of ABT-510 is 30% in subcutaneous injection[37]. The transportation between the subcutaneous and blood compartments is unidirectional and is assumed to occur at the same as the rate transport between the normal and blood compartments. The degradation rate of ABT-510 follows its measured circulation half-time in the human body (1.2 hours). ABT-510 binds to TSP1 receptor CD36 to induce an anti-angiogenic signal[38] (***Fig. 1G***). Since ABT-510 is a TSP1-derived peptidomimetic, we assume it has the same affinity to CD36 as TSP1.

2.4 Quantification of Combination Effect

Commonly used dose–effect-based approaches to quantify drug combination effects rely on the mathematical framework known as Loewe Additivity[39]. It calculates the combination of dose *a* for drug *X* and dose *b* for drug *Y* that can produce the same effect as dose *A* of drug *X* alone and dose *B* of drug *Y* alone. The combination effect of drug *X* and drug *Y* can be expressed as:

$$\frac{a}{A} + \frac{b}{B} = CI$$

where *CI* is the combination index. We evaluate the combination effect (*Fc*) of 10 mg/kg of bevacizumab and 100 mg of ABT-510. Thus, *a* = 10 mg/Kg and *b* = 100 mg. We change the doses of bevacizumab and ABT-510 to get the dose-effect curve of single-agent treatments and find the Dose *A* and Dose *B* corresponding to *Fc*. A *CI* less than one indicates synergy between the two drugs, a *CI* equal to one represents simple additivity, and *CI* greater than one indicates antagonism.

2.5 Partial Least Squares Regression

Partial least squares regression (PLSR) relates input variables to output variables by maximizing the correlation between the variables. This is accomplished by projecting the output variables onto new dimensions (principal components, PCs), which are linear combinations of the inputs. We use PLSR to investigate the relationship between tumor receptor numbers and the response to anti-angiogenic therapy (the fold-change in the angiogenic ratio in the tumor tissue, termed *F*). The PLSR model is trained and validated with the 1,000 different combinations of tumor receptor densities (inputs) and the corresponding responses to treatment generated by the three-compartment systems biology model (outputs). The receptor values are normalized by dividing by the lower bound of the sampling range. Since the receptor numbers are sampled from a uniform distribution within 10-fold above and below the baseline value, the normalized receptor values range from 1 to 100. The nonlinear iterative partial least squares (NIPALS) algorithm was used to implement the PLSR analysis[40]. Leave-one-out cross validation is applied to quantify the predictive capability of the PLSR model. Furthermore, we calculated the "variable importance of projection" (VIP) for each input variable[41], which is the weighted sum of each input's contribution to the output. As such, the VIP evaluates the overall importance of an input variable in predicting the output. VIP values greater than one indicate variables that are important for predicting the output response.

3. Results:

3.1 Angiogenic balance is predicted to shift during combination therapy

We apply the compartmental model to predict how the angiogenic signal changes with anti-angiogenic treatment. We simulate one cycle (14 days) of combination therapy, following the protocol used in clinical trial[20]. Bevacizumab was given at a dose of 10 mg/kg through intravenous infusion lasting 90 minutes. ABT-510 was administered at 100 mg every 12 hours for 14 days. The concentrations of unbound ("free") VEGF and TSP1 over time, along with dynamics of the "angiogenic ratio", are reported to show the change of angiogenic signals during combination therapy (***Fig. 2***). The angiogenic ratio is the number of pro-angiogenic complexes over the number of anti-angiogenic complexes (see ***Methods***). If the angiogenic ratio is greater than one, the compartment is considered to be in a pro-angiogenic state.

After one cycle of the combination therapy, the concentration of free VEGF is predicted to decrease in all three compartments (***Fig. 2A***). The tumor VEGF level changes from 149 pM to 14 pM after one treatment cycle. The levels of free VEGF in plasma and normal tissue decreased from 1.6 pM to 1.2 pM and from 1.0 pM to 0.9 pM, respectively. In contrast, the free

active TSP1 level in all three compartments is highly stable throughout the whole treatment cycle (***Fig. 2B***), remaining at 117 pM, 96 pM, and 66 pM in the tumor, blood, and normal compartments, respectively. This indicates that the combination therapy does not affect the free TSP1 level in human body. The experimental measurements from clinical study also show that the level of TSP1 does not significantly change[20], which validates this prediction. However, the combination therapy is predicted to significantly reduce the angiogenic ratio in all compartments. Before treatment, the angiogenic ratio (***Fig. 2C***) is predicted to highly favor angiogenesis in tumor and blood, where the ratios are 14.4 and 6.2, respectively. In comparison, the angiogenic ratio is almost balanced in the rest of the body (1.3 in normal compartment). The values of the angiogenic ratios at the end of the treatment cycle are 6.6, 2.0, and 0.6 in the tumor, blood, and normal compartments. Thus, following treatment, the angiogenic balance is significantly reduced but still favors angiogenesis in tumor tissue and blood and opposes angiogenesis in normal tissue. In all compartments, the angiogenic ratio is predicted to oscillate during the treatment. Since the ABT-510 drug has a short half-life (1.2 hours in circulation), it requires a high frequency of administration (twice-daily injections), which causes the angiogenic ratio to oscillate following each injection. Specifically, the angiogenic ratio decreases to a low level for a short time after the administration of ABT-510 and goes back to a medium level before the next dose of ABT-510.

To get detailed insight into how the angiogenic ratio varies, we report the change of all the tumor angiogenic complexes in combination therapy and single agent treatment (***Supplementary Fig. S2***). VEGF can bind to four different receptors, including VEGF receptor 1 (R1), VEGF receptor 2 (R2), neuropilin-1 (N1) and neuropilin-2 (N2). Thus, four different types of pro-angiogenic complexes are formed. TSP1 binds to four different receptors, including CD47, CD36, LRP1 and β1) to produce four types of anti-angiogenic complexes. Our predictions show that bevacizumab promotes a decrease in the pro-angiogenic complex involving VEGFR1 (***Fig. S2A***) and ABT-510 drives an increase in the anti-angiogenic complex involving CD36 (***Fig. S2B***). The absolute levels of other angiogenic complexes only show small changes. The effect of the two agents in combination on the formation of angiogenic complexes is a superimposition of their individual effects (***Fig. S2C***).

3.2 Therapeutic response varies due to tumor receptor heterogeneity

To examine the impact of tumor receptor heterogeneity, we varied the number of VEGF and TSP1 receptors in the tumor tissue (both on tumor cells and diseased endothelial cells). We set

the density of each receptor by sampling within two orders of magnitude of the baseline value. This variability in the receptor number influences the dynamics of free VEGF, free TSP1, and the angiogenic ratio, as shown in ***Supplementary Fig. S3***. We use the "fold-change" of free VEGF, free TSP1, and the angiogenic ratio to characterize the response to combination treatment. The fold-change is the post-treatment level compared to the pre-treatment level. When the fold-change is less than one, the quantity has decreased after treatment. We further define a therapeutic response to be when the fold-change of free VEGF or the angiogenic ratio is less than one. The model predicts that combination treatment elicits a therapeutic effect for all of the receptor levels simulated. That is, the fold-change of free VEGF and the angiogenic ratio are predicted to be lower than one in all three compartments (***Fig. 3A***), indicating that free VEGF and the angiogenic ratio decrease after treatment.

Model predictions show that the response level of the fold-change in tumor varies depending on the tumor receptor profile. Different combinations of sampled parameter values represent patients with different tumor receptor profiles. The model predicts a wide range of fold-changes for the angiogenic ratio and free VEGF in the tumor compartment (***Fig. 3A***), which indicates that different tumor receptor profiles lead to different responses to the combination therapy. Furthermore, the skewed distribution of the fold-changes of the tumor angiogenic ratio (F) (***Fig. 3B, orange***) shows that the majority (83%) of the sampled tumor profiles lead to intermediate responses with fold-change ranging from 0.5 to 1. A smaller percentage of profiles (17%) have a strong response to treatment ($F < 0.5$). Interestingly, there are some outliers for which combination treatment significantly decreases the pro-angiogenic signal, with fold-changes of free VEGF or angiogenic ratio much lower than one. These results imply that particular tumor receptor profiles could have a strong therapeutic response to combination therapy. In single-agent anti-angiogenic tumor therapy (ABT-510 or bevacizumab treatment alone), heterogeneous responses are also observed (***Fig. 3B, green and purple***). Thus, the response to single-agent treatment also varies depending on the tumor receptor profile.

Tumor receptor heterogeneity influences treatment outcomes in other aspects. Firstly, variability in the tumor receptor numbers could affect the targeting of combination anti-angiogenic therapy. Our simulations show combination therapy is not always efficiently targeting tumor angiogenesis. For most cases, the fold-change of the angiogenic ratio in healthy tissue and in blood is lower than in the tumor (***Fig. 3A***). This indicates treatment is more effective in shifting the angiogenic balance in healthy tissue rather than in the tumor. For these tumor patients, the combination

therapy is targeting physiological angiogenesis instead of tumor angiogenesis. Interestingly, this insight is not captured by solely examining the fold-change of VEGF. Secondly, tumor receptor heterogeneity influences the effect of combination therapy on individual angiogenic pathways. The model predicts that the fold-change of the VEGFR2- and neuropilin-1-containing pro-angiogenic complexes in tumor could be higher than one for some sampled cases (***Supplementary Fig. S4***). This indicates that for some tumor receptor profiles, the pro-angiogenic signaling pathway of VEGFR2 or NRP-1 will be enhanced after treatment instead of inhibited. Similar results are seen when simulating bevacizumab treatment (data not shown). Interestingly, these unintended outcomes following bevacizumab treatment predicted by the model have been observed clinically: a substantial increase in phosphorylated VEGFR2[42] and variable changes in phosphorylated VEGFR2 in the clinical trial of the combination anti-angiogenic therapy[20].

3.3 Tumor receptor heterogeneity affects the combination effect

We used the model to compare the response to single- and dual-agent therapy and find that the response to combination therapy is related to the response to single-agent treatment (***Fig. 4A***). The color changes from red to yellow along the diagonal direction (from upper right to lower left) shows that the response to combination treatment (*Fc*) improves when the response to either single-agent treatment is higher. This indicates that a better response to single-agent treatment may correspond to a better response to combination therapy. We then examined the superiority of the drug combination compared to the single agents. The color of the points in ***Fig. 4B*** indicates the difference between the response to combination therapy and the best response amongst the two single-agent treatments. Although this difference changes depending on the tumor receptor profile, for all sampled cases, the difference is higher than zero. This indicates that the response to combination therapy is better than single agent treatment. Thus, if only considering the fold-change of tumor angiogenic ratio (*F*), the combination therapy of bevacizumab and ABT-510 is superior to single-agent therapy for all of the sampled tumor receptor profiles.

We explicitly calculated the combination effect to determine if the action of the two drugs is synergistic or additive. We selected four sets of tumor receptor profiles (***Fig. 4A***, triangles) and calculated the combination index (*CI*) of the Loewe additivity (see ***Methods***). These are representative cases corresponding to patients that respond well to ABT-510 alone (“1”), bevacizumab alone (“2”), or combination therapy (“3”), and one patient that does not respond

well to either drug ("4"). The calculated *CI* values are different for these four tumor profiles (***Fig. 4C***), where the combination effect could be synergistic (i.e., patient 3 with *CI* = 0.65) or nearly additive (i.e., patients 1 and 2 have *CI* = 0.89; patient 4 has *CI* = 0.97). Thus, the combination effect of bevacizumab and ABT-510 is also affected by tumor receptor heterogeneity.

3.4 Therapeutic response depends on tumor cell VEGFR1, CD36 and CD47 expression

Given the observed impact of tumor receptor heterogeneity in the predictions from the mechanistic model, we explored if we can use tissue biomarkers (tumor receptor levels) to determine the response to combination anti-angiogenic therapy *a priori*. We used partial least squares regression (PLSR) to characterize the association between tumor receptor levels and the response to combination therapy (the fold-change in the angiogenic ratio in the tumor). Specifically, we established a predictive PLSR model that estimates the response to combination therapy using the tumor angiogenic receptor profile (***Supplementary Fig. S5A***). We used 18 variables as the inputs in PLSR modeling, including the 16 VEGF and TSP1 receptor numbers on diseased endothelial cells and tumor cells that were varied, and two nonlinear terms comprised of ratios of receptor numbers. The fold-changes estimated by the PLSR model closely match the actual values given by the mechanistic model (the points lie along the 45°-angle line). The high Q^2Y value of 0.94, indicates that in leave-one-out cross validation, the PLSR model predicts over 94% of the total variation in the fold-change of tumor angiogenic ratio. The R^2Y value of 0.93 shows the most of the variation in the response is also captured by the PLSR model, while the R^2X value indicates that only a small portion of the receptor information (15%) is useful for predicting the therapeutic response.

The variable importance of projection (VIP) score was calculated to find which variables, across the entire PLSR model, most significantly contribute to determining the response to combination therapy[41]. VEGFR1, CD36 and CD47 levels on tumor cells were found to be important for explaining the response, as they have VIP scores higher than one (***Fig. 5A***). The two nonlinear terms of tumor cell receptor numbers are also identified as important variables. We found that all of the receptors on tumor endothelial cells have VIP score lower than 0.5, indicating that tumor endothelial cell receptor expression was not as influential as receptor expression on tumor cells in predicting the response to combination therapy. Plotting the values of the receptors with VIP scores greater than one versus the response to combination therapy shows that lower VEGFR1 expression, lower CD47 expression and higher CD36 expression on tumor cells correlate with higher response (***Fig. 5B-D***). This indicates the patients with low tumor cell

VEGFR1 or CD47 expression or high tumor cell CD36 expression are likely to show a stronger response to combination therapy than others. The associations between response and other receptors are not pronounced (***Supplementary Fig. S6***). The therapeutic response is also related to the two nonlinear terms in a monotonic fashion (***Fig. 5E-F***). Interestingly, although the response to treatment exhibits a trend that correlates with certain individual receptors, the data highly deviates from the LOWESS smoothing of the data (***Fig. 5, black lines***). This indicates that none of the 16 receptor variables can accurately predict the response alone, and the variability in the expression of a single receptor cannot account for all of the variability in the response to combination anti-angiogenic therapy.

4. Discussion:

The investigation of anti-angiogenic therapy greatly benefits from computational models that provide quantitative insight into the heterogeneous responses to therapy. In the present study, we constructed a novel whole-body model that incorporates ligand-receptor interactions of VEGF and TSP1, two important regulators of angiogenesis. This model enables the study of the combination anti-angiogenic therapy that systematically targets the angiogenic balance as a whole. Here, we simulated the combination of bevacizumab and ABT-510 and investigate how tumor receptor heterogeneity influences the response to treatment. In addition to illustrating the impact of tumor receptor heterogeneity, there are many applications of our model, including identifying potential biomarkers that predict the response to treatment, providing mechanistic insight into experimental and clinical observations, and optimizing anti-angiogenic strategies.

This work uses a molecular-based pharmacokinetic model to bridge the heterogeneous response of anti-angiogenic therapy with tumor receptor heterogeneity. Tumor angiogenic receptor heterogeneity has been observed in various settings. Qualitative information on the differential expression of angiogenic receptors from different tumor samples is reported in Human Protein Atlas Database[26,27]. Quantitative measurements also show the cell-to-cell variations in the density of VEGF receptors across different cell lines[24,25]. This heterogeneity is thought to influence prognosis and response to treatment, which has been validated experimentally. The VEGFR2 heterogeneity was proved to influence the response to an anti-angiogenic cyclophosphamide treatment in a pre-clinical model[43]. The inter-patient VEGFR1 and neuropilin heterogeneity has been associated with the response to bevacizumab treatment in search for biomarkers[44,45]. To complement the preclinical and clinical studies, this work

provides a possible quantitative characterization of the mechanisms leading to the clinically observed heterogeneous responses to combination anti-angiogenic therapy[7,11,46]. The model predicts that after one cycle of treatment, the fold-change of the angiogenic ratio in tumor tissue varies widely depending on the tumor receptor levels, which indicates tumor receptor heterogeneity could contribute to heterogeneous response and should be considered when developing more effective and personalized anti-angiogenic therapy.

The work helps identify biomarkers that predict response to anti-angiogenic treatment. The heterogeneous response to anti-angiogenic therapy is a major drawback not limited to the combination therapy of bevacizumab and ABT-510, but generally to all anti-angiogenic agents[7,46]. However, despite substantial research[47], there is currently no reliable biomarker for identifying patients for which anti-angiogenic therapy will be effective. The PLSR analysis in our study showed that the levels of CD36, CD47, and VEGFR1 on tumor cells are potential biomarkers to select the patients who will likely respond to combination treatment. These receptors are shown to have a pronounced impact on the response: low expression of VEGFR1 and CD47 and high expression of CD36 all associate with high response to combination treatment. Interestingly, the relationship between VEGFR1 and the effect of bevacizumab has also been observed in clinical trial. Fountzilas *et al.* report that intra-tumoral VEGFR1 overexpression was an indicator for poor survival in metastatic breast cancer patients receiving bevacizumab and chemotherapy[48], supporting the finding in our study. In addition to identifying these biomarkers, our study emphasizes the importance of the integration of information from multiple receptors to accurately predict the response. We showed that the expression of a single receptor is not able to fully account for the heterogeneous response to therapy. Instead, a comprehensive analysis that incorporates multiple biomarkers is more appropriate. In the experimental and clinical practice of biomarker discovery, it is commonly accepted that a single biomarker is not able to predict anti-angiogenic treatment efficacy[47]. Our findings support this stance and demonstrate that a computational approach could help identify biomarkers by providing systematic understanding of the response to treatment.

Given the molecular detail of the model, we gain mechanistic insight into the model predictions. For example, we can understand how the individual tumor receptor populations change in response to anti-angiogenic therapy, insight that explains why VEGFR1, CD36, and CD47 are potential biomarkers. VEGFR1 has been supported as a possible *in situ* predictive biomarker for anti-VEGF agents in both preclinical and clinical settings[47–49]. Our model predicts that the pro-

angiogenic complexes involving VEGFR1 have the most more important role in the response to bevacizumab treatment. The pro-angiogenic complexes involving VEGFR1 significantly decrease after the administration of bevacizumab while the levels of other angiogenic complexes are relatively stable before and after bevacizumab treatment. The high expression of VEGFR1 can efficiently compete for VEGF, thereby limiting the benefits of VEGF neutralization through bevacizumab. On the other side, high expression of CD36 provides more available receptors for ABT-510 to bind to, which enables the formation of more anti-angiogenic complexes to shift the angiogenic balance. Since CD47 has a high affinity for TSP1, increasing the expression of CD47 will significantly elevate the baseline level of anti-angiogenic complexes. This means that the tumor has a higher baseline anti-angiogenic signal and consequently shows an attenuated response to the benefit of forming more anti-angiogenic complexes through ABT-510. The insights generated by our model can guide future experimental or clinical studies of predictive biomarkers for anti-angiogenic treatment.

The predictions of our model also provide insight into outcomes from clinical trials involving anti-angiogenic agents. ABT-510 failed in Phase II clinical trials for advanced renal cell carcinoma and metastatic melanoma[16,17]. According to our model simulations, low CD36 expression on tumor cell could lead to the low observed response to ABT-510. Interestingly, the Human Protein Atlas shows CD36 is not detected in human renal cancer samples (in 10 out of 10 samples) and melanoma samples (in 11 out of 11 samples)[27]. The heterogeneous expression of CD36 might be a possible reason for the failure of ABT-510. In the combination of bevacizumab and ABT-510 for advanced solid tumors, only 32% percent of the patients have prolonged stable disease for more than 6 months[20], which shows no evidence of being better than bevacizumab alone. Our model predicts that the difference between combination therapy and the best response of individual bevacizumab or ABT-510 treatment will become zero when the response to ABT-510 is very low. This means that the combination will not be superior to bevacizumab if ABT-510 alone is highly ineffective, which provides a possible explanation for the clinical observations.

Although we specifically simulate the combination of bevacizumab and ABT-510 in this work, our model can be adapted to study other anti-angiogenic agents that target VEGF and TSP1 signaling and help explore different anti-angiogenic strategies. Given the many different anti-angiogenic agents[7,15] and possible drug regimens, our realistic model could be a valuable help in the search for the optimal combination anti-angiogenic strategy. Additionally, this model has

practical interest, which can help circumvent difficulty in experimental studies. Traditional experiment-based study of comparing the effects of combination therapy to individual agents is limited by the difficulty of accumulating enough data to make meaningful comparisons. In contrast, our model can easily simulate multiple anti-angiogenic treatment strategies and quantitatively evaluate the added benefit of combination therapy as compared to single-agent therapy. In this study, we show that the combination of bevacizumab and ABT-510 leads to a better response than administering either agent alone, in all of the sampled cases. However, the combination index revealed that the combination of these two drugs does not always have a strong synergistic effect, due to tumor receptor expression. This information underlines the need to consider tumor receptor heterogeneity in the design of drug combination strategies. Our model might help identify drug regimens that take advantage of the synergy and aids the design of anti-angiogenic therapy in order to achieve high efficacy with low drug dosage.

We acknowledge some limitations of the model that can be addressed in future studies. In this study, we use the angiogenic ratio to represent the angiogenic state, assuming that each angiogenic complex equally contributes to angiogenesis. However, it is known that the angiogenic receptors have unique functions and influence angiogenesis in different ways. For example, VEGFR1 primarily modulates blood vessel angiogenesis by ligand-trapping and receptor dimerization, while VEGFR2 is the predominant receptor that promotes pro-angiogenic VEGF signaling pathways[50,51]. On the anti-angiogenic side, CD36 and CD47 are reported to inhibit angiogenesis by antagonizing survival pathways and activating apoptotic pathways[52]. This knowledge of the relevant intracellular signaling pathways can be combined with our model to study specific functional responses to anti-angiogenic therapy. Secondly, it is worth noting that there are alternate ways of characterizing the magnitude of the response to anti-angiogenic therapy. We focus on the angiogenic ratio, where the balance of pro- and anti-angiogenic factors has been experimentally shown to be a more accurate approach to study angiogenesis than analyzing the level of angiogenic factors individually[53]. We further calculate the fold-change of the angiogenic ratio to characterize the response to anti-angiogenic treatment, while the area under the angiogenic ratio curve for the tumor compartment could be an alternative way to quantify the response to treatment. In that case, the response to ABT-510 is more substantial due to the strong shifting of the angiogenic ratio in the short time after each bolus (data not shown). However, the conclusions of our study remain unchanged. Another metric to consider is whether anti-angiogenic treatment shifts the angiogenic balance in tumor to the level observed in healthy tissue, related to vessel normalization[54]. Since a universal definition of the response

to anti-angiogenic therapy is still missing, the fold-change of the angiogenic balance of pro- and anti-angiogenic receptor complexes remains as an important indicator, which this research is well suited to address.

Concluding thoughts. Our model illustrates the effect of combination therapy of bevacizumab and ABT-510 on changing the balance between two opposing angiogenic signals. The model provides a quantitative description of the impact of tumor receptor heterogeneity on the response to combination anti-angiogenic therapy and aids in the discovery of predictive biomarkers. We expect that the insights generated by our model predictions will shed light on previously obscure clinical observations and that the model will be used to facilitate the optimization of new clinical trials.

Acknowledgements

The authors thank members of the Finley research group for critical comments and suggestions.

References:

1. Mac Gabhann F, Ji JW, Popel AS. Multi-scale computational models of pro-angiogenic treatments in peripheral arterial disease. *Ann Biomed Eng*. 2007;35(6):982-994.
2. Faeder JR, Blinov ML, Hlavacek WS. Rule-based modeling of biochemical systems with BioNetGen. *Methods Mol Biol*. 2009;500(1):113-167. doi:10.1007/978-1-59745-525-1_5.
3. Kaur S, Martin-Manson G, Pendrak ML, Garfield SH, Isenberg JS, Roberts DD. Thrombospondin-1 inhibits VEGF receptor-2 signaling by disrupting its association with CD47. *J Biol Chem*. 2010;285(50):38923-38932.
4. Chu LY, Ramakrishnan DP, Silverstein RL. Thrombospondin-1 modulates VEGF signaling via CD36 by recruiting SHP-1 to VEGFR2 complex in microvascular endothelial cells. *Blood*. 2013;122(10):1822-1832. doi:10.1182/blood-2013-01-482315.
5. Hanahan D, Wienberg RA. Hallmarks of cancer: the next generation. *Cell*. 2011;144(5):646-674.
6. Nishida N, Yano H, Nishida T, Kamura T, Kojiro M. Angiogenesis in cancer. *Vasc Health Risk Manag*. 2006;2(3):213-219. doi:10.2147/vhrm.2006.2.3.213.
7. Vasudev NS, Reynolds AR. Anti-angiogenic therapy for cancer: Current progress, unresolved questions and future directions. *Angiogenesis*. 2014;17(3):471-494.

doi:10.1007/s10456-014-9420-y.

8. Hanahan D, Folkman J. Patterns and emerging mechanisms of the angiogenic switch during tumorigenesis. *Cell*. 1996;86(3):353-364. doi:10.1016/S0092-8674(00)80108-7.
9. Sakurai T, Kudo M. Signaling pathways governing tumor angiogenesis. *Oncology*. 2011;81(supp 1):24-29.
10. Huang Z, Bao SD. Roles of main pro- and anti-angiogenic factors in tumor angiogenesis. *World J Gastroenterol*. 2004;10(4):463-470. doi:10.3748/wjg.v10.i4.463.
11. Wehland M, Bauer J, Infanger M, Grimm D. Target-based anti-angiogenic therapy in breast cancer. *Curr Pharm Des*. 2012;18(27):4244-4257. doi:10.2174/138161212802430468.
12. Ren B, Yee KO, Lawler J, Khosravi-Far R. Regulation of tumor angiogenesis by thrombospondin-1. *Biochim Biophys Acta*. 2006;1765(2):178-188. doi:DOI 10.1016/j.bbcan.2005.11.002.
13. Lawler J. Thrombospondin-1 as an endogenous inhibitor of angiogenesis and tumor growth. *J Cell Mol Med*. 2002;6(1):1-12. doi:006.001.01 [pii].
14. Armstrong LC, Bornstein P. Thrombospondins 1 and 2 function as inhibitors of angiogenesis. In: *Matrix Biology*. Vol 22. ; 2003:63-71. doi:10.1016/S0945-053X(03)00005-2.
15. Jeanne A, Schneider C, Martiny L, Dedieu S. Original insights on thrombospondin-1-related antireceptor strategies in cancer. *Front Pharmacol*. 2015;6:252. doi:10.3389/fphar.2015.00252.
16. Markovic SN, Suman VJ, Rao RA, et al. A phase II study of ABT-510 (thrombospondin-1 analog) for the treatment of metastatic melanoma. *Am J Clin Oncol*. 2007;30(3):303-309. doi:10.1097/01.coc.0000256104.80089.35.
17. Ebbinghaus S, Hussain M, Tannir N, et al. Phase 2 study of ABT-510 in patients with previously untreated advanced renal cell carcinoma. *Clin Cancer Res*. 2007;13(22 Pt 1):6689-6695. doi:10.1158/1078-0432.CCR-07-1477.
18. Yadav L, Puri N, Rastogi V, Satpute P, Sharma V. Tumour angiogenesis and angiogenic inhibitors: A review. *J Clin Diagnostic Res*. 2015;9(6):XE01-XE05. doi:10.7860/JCDR/2015/12016.6135.
19. Bergers G, Benjamin LE. Angiogenesis: Tumorigenesis and the angiogenic switch. *Nat Rev Cancer*. 2003;3(6):401-410. doi:10.1038/nrc1093.
20. Uronis HE, Cushman SM, Bendell JC, et al. A phase I study of ABT-510 plus bevacizumab in advanced solid tumors. *Cancer Med*. 2013;2(3):316-324.

doi:10.1002/cam4.65.

21. Finley SD, Chu L-H, Popel AS. Computational systems biology approaches to anti-angiogenic cancer therapeutics. *Drug Discov Today*. 2015;20(2):187-197.
22. Stefanini MO, Wu FTH, Mac Gabhann F, Popel AS. Increase of plasma VEGF after intravenous administration of bevacizumab is predicted by a pharmacokinetic model. *Cancer Res*. 2010;70(23):9886-9894. doi:10.1158/0008-5472.CAN-10-1419.
23. Rohrs JA, Sulistio CD, Finley SD. Predictive model of thrombospondin-1 and vascular endothelial growth factor in breast tumor tissue. *Npj Syst Biol Appl*. 2016;2:16030.
24. Imoukhuede PI, Popel AS. Quantitative fluorescent profiling of VEGFRs reveals tumor cell and endothelial cell heterogeneity in breast cancer xenografts. *Cancer Med*. 2014;3(2):225-244. doi:10.1002/cam4.188.
25. Imoukhuede PI, Popel AS. Quantification and cell-to-cell variation of vascular endothelial growth factor receptors. *Exp Cell Res*. 2011;317(7):955-965.
26. Uhlen M, Fagerberg L, Hallstrom BM, et al. Tissue-based map of the human proteome. *Science (80-)*. 2015;347(6220):1260419-1260419. doi:10.1126/science.1260419.
27. Uhlen M. A Human Protein Atlas for Normal and Cancer Tissues Based on Antibody Proteomics. *Mol Cell Proteomics*. 2005;4(12):1920-1932. doi:10.1074/mcp.M500279-MCP200.
28. Finley SD, Popel AS. Effect of tumor microenvironment on tumor VEGF during anti-VEGF treatment: systems biology predictions. *J Natl Cancer Inst*. 2013;105(11):802-811.
29. Byrne GJ, Hayden KE, McDowell G, et al. Angiogenic characteristics of circulating and tumoural thrombospondin-1 in breast cancer. *Int J Oncol*. 2007;31(5):1127-1132.
30. Baker EA, Leaper DJ, Hayter JP, Dickenson AJ. The matrix metalloproteinase system in oral squamous cell carcinoma. *Br J Oral Maxillofac Surg*. 2006;44(6):482-486. doi:10.1016/j.bjoms.2005.10.005.
31. Kut C, Mac Gabhann F, Popel AS. Where is VEGF in the body? A meta-analysis of VEGF distribution in cancer. *Br J Cancer*. 2007;97(7):978-985.
32. Vasaturo F, Solai F, Malacrino C, et al. Plasma levels of matrix metalloproteinases 2 and 9 correlate with histological grade in breast cancer patients. *Oncol Lett*. 2012;5(1):316-320. doi:10.3892/ol.2012.977.
33. Hoier B, Passos M, Bangsbo J, Hellsten Y. Intense intermittent exercise provides weak stimulus for vascular endothelial growth factor secretion and capillary growth in skeletal muscle. *Exp Physiol*. 2013;98(2):585-597. doi:10.1113/expphysiol.2012.067967.
34. Gordon MS, Margolin K, Talpaz M, et al. Phase I safety and pharmacokinetic study of

recombinant human anti-vascular endothelial growth factor in patients with advanced cancer. *J Clin Oncol*. 2001;19(3):843-850.

35. Kagan L. Pharmacokinetic modeling of the subcutaneous absorption of therapeutic proteins. *Drug Metab Dispos*. 2014;42(11):1890-1905. doi:10.1124/dmd.114.059121.
36. Hoekstra R, de Vos FYFL, Eskens FALM, et al. Phase I safety, pharmacokinetic, and pharmacodynamic study of the thrombospondin-1-memetic angiogenesis inhibitor ABT-510 in patients with advanced cancer. *J Clin Oncol*. 2005;23(22):5188-5197.
37. Jensen JD, Jensen LW, Madsen JK. The pharmacokinetics of recombinant human erythropoietin after subcutaneous injection at different sites. *Eur J Clin Pharmacol*. 1994;46(4):333-337. doi:10.1007/BF00194401.
38. Anderson JC, Grammer JR, Wang W, et al. ABT-510, a modified type 1 repeat peptide of thrombospondin, inhibits malignant glioma growth in vivo by inhibiting angiogenesis. *Cancer Biol Ther*. 2007;6(3):454-462. doi:10.4161/cbt.6.3.3630.
39. Foucquier J, Guedj M. Analysis of drug combinations : current methodological landscape. 2015. doi:10.1002/prp2.149.
40. Geladi P, Kowalski BR. Partial least-squares regression: a tutorial. *Anal Chim Acta*. 1986;185:1-17.
41. Kreeger PK. Using partial least squares regression to analyze cellular response data. *Sci Signal*. 2013;6(271):tr7.
42. Wedam SB, Low JA, Yang SX, et al. Antiangiogenic and antitumor effects of bevacizumab in patients with inflammatory and locally advanced breast cancer. *J Clin Oncol*. 2006;24(5):769-777. doi:10.1200/JCO.2005.03.4645.
43. Patten SG, Adamcic U, Lacombe K, Minhas K, Skowronski K, Coomber BL. VEGFR2 heterogeneity and response to anti-angiogenic low dose metronomic cyclophosphamide treatment. *BMC Cancer*. 2010;10:683. doi:10.1186/1471-2407-10-683.
44. Jubb AM, Miller KD, Rugo HS, et al. Impact of exploratory biomarkers on the treatment effect of bevacizumab in metastatic breast cancer. *Clin Cancer Res*. 2011;17(2):372-381.
45. Van Cutsem E, de Haas S, Kang Y-K, et al. Bevacizumab in combination with chemotherapy as first-line therapy in advanced gastric cancer: A biomarker evaluation from the AVAGAST randomized Phase III trial. *J Clin Oncol*. 2012;30(17):2119-2127.
46. Moserle L, Jiménez-Valerio G, Casanovas O. Antiangiogenic therapies: Going beyond their limits. *Cancer Discov*. 2014;4(1):31-41. doi:10.1158/2159-8290.cd-13-0199.
47. Wehland M, Bauer J, Magnussion NE, Infanger M, Grimm D. Biomarkers for anti-angiogenic therapy in cancer. *Int J Mol Sci*. 2013;14(5):9338-9364.

48. Fountzilas G, Kourea HP, Bobos M, et al. Paclitaxel and Bevacizumab as First Line Combined Treatment in Patients with Metastatic Breast Cancer : The Hellenic Cooperative Oncology Group Experience with Biological Marker Evaluation. 2011;3018:3007-3018.
49. Lambrechts D, Lenz H-J, de Haas S, Carmeliet P, Scherer SJ. Markers of response for the antiangiogenic agent bevacizumab. *J Clin Oncol*. 2013;31(9):1219-1230.
50. Shibuya M. Vascular Endothelial Growth Factor (VEGF) and Its Receptor (VEGFR) Signaling in Angiogenesis: A Crucial Target for Anti- and Pro-Angiogenic Therapies. *Genes Cancer*. 2011;2(12):1097-1105. doi:10.1177/1947601911423031.
51. Rahimi N. VEGFR-1 and VEGFR-2: two non-identical twins with a unique physiognomy. *Front Biosci*. 2006;11:818-829. doi:10.2741/1839.
52. Lawler PR, Lawler J. Molecular basis for the regulation of angiogenesis by thrombospondin-1 and -2. *Cold Spring Harb Perspect Med*. 2012;2(5):a006627.
53. Roudier E, Gineste C, Wazna A, Dehghan K, Desplanches D, Birot O. Angio-adaptation in unloaded skeletal muscle: new insights into an early and muscle type-specific dynamic process. *J Physiol*. 2010;588(22):4579-4591. doi:10.1113/jphysiol.2010.193243.
54. Jain RK. Normalizing tumor microenvironment to treat cancer: Bench to bedside to biomarkers. *J Clin Oncol*. 2013;31(17):2205-2218.

Tables

Table 1. Comparison of predicted and experimental steady state concentrations of VEGF, TSP1 and MMPs.

Species	Range of Experimental Measurements*	Predicted Concentration	Source and References
Tumor Tissue			
VEGF	8.0-389 pM	148.6 pM	Multiple cancer types[28]
TSP1[#]	1.0-6.2 nM (2.0)	2.0 nM	Breast cancer patients[29]
MMP3	1.8-65.1 nM (5.1)	4.9 nM	Oral squamous cell carcinoma[30]
MMP9 total	1.0-287.8 nM (9.0)	9.3 nM	Oral squamous cell carcinoma[30]
MMP9 active	0-22.4 nM (0.8)	0.2 nM	Oral squamous cell carcinoma[30]
Plasma			
VEGF	0.4-3.0 pM	1.6 pM	Multiple cancer types[31]
TSP1[#]	0.8-2.1 nM (1.2)	1.2 nM	Breast cancer patients[29]
MMP3	1.9-2.0 nM	1.9 nM	Breast cancer patients[32]
MMP9 total	0.6-0.7 nM	0.7 nM	Breast cancer patients[32]
Normal Tissue			
VEGF	0.3-3.0 pM	1.0 pM	Heathy subjects[28]
TSP1[#]	0.2 nM	0.9 nM	Heathy subjects[33]
MMP3	0.9-66.4 nM (4.1)	4.2 nM	Oral squamous cell carcinoma[30]
MMP9 total	0.8-27.7 nM (5.0)	3.2 nM	Oral squamous cell carcinoma[30]
MMP9 active	0-4.1 nM (0.02)	0.05 nM	Oral squamous cell carcinoma[30]

* Median value is shown in parentheses, if provided in literature. If the experimental data reflects the total concentration in tissue, we assume 50% of the total protein amount is localized in extracellular space.

TSP1 concentration includes both the active TSP1 and the cleaved TSP1.

Figures and captions:

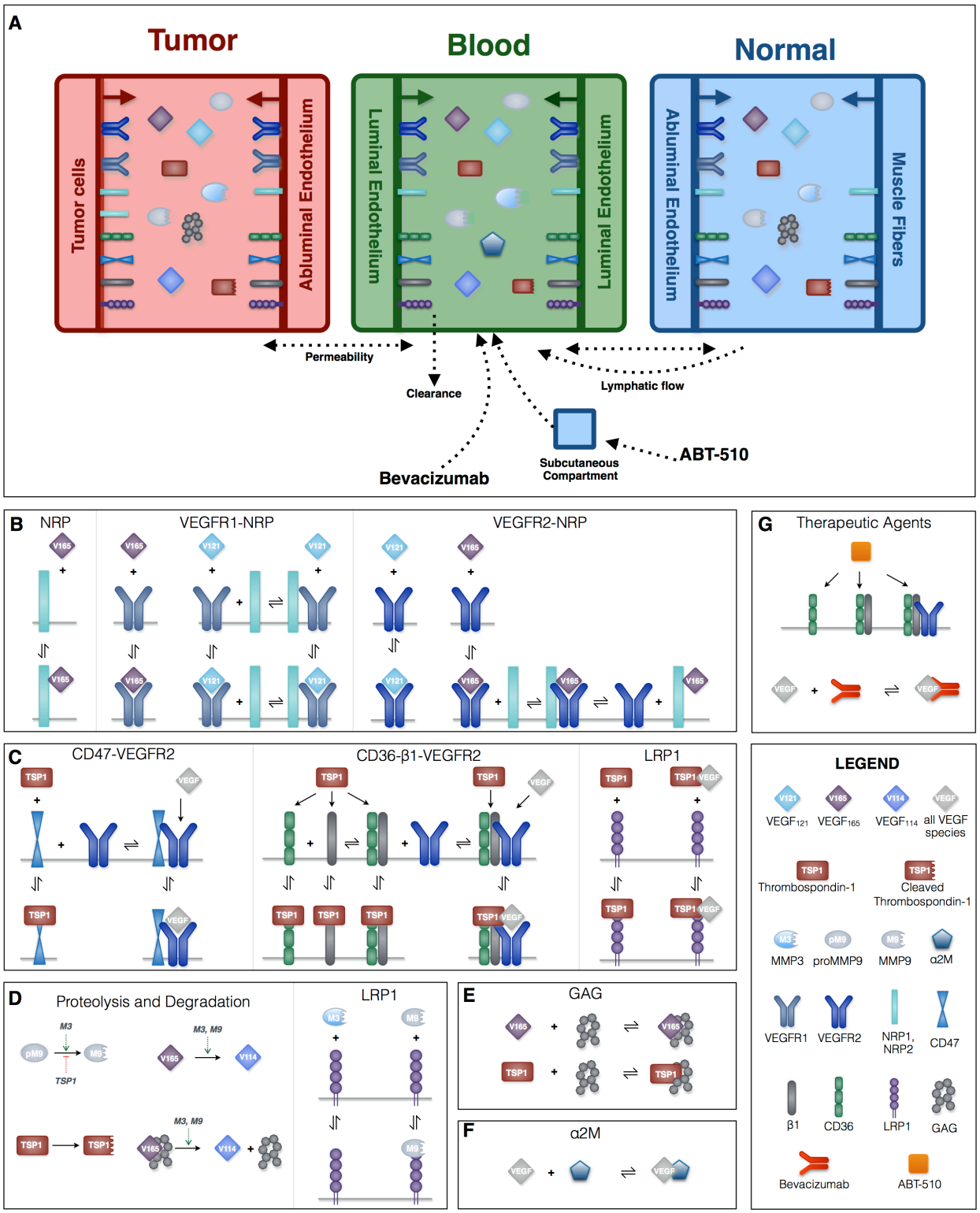

Figure 1. Compartmental model of VEGF-TSP1 system in human cancer patient and TSP1 and VEGF interactions. (A) The model includes three compartments: normal tissue, blood, and tumor tissue. The endothelial cells and parenchymal cells secrete soluble species (VEGF, MMP3, proMMP9 and TSP1) into the compartments. Receptors are localized on the luminal and abluminal surfaces of endothelial and parenchymal cells. Free and ligand-bound receptors can be internalized. Transport between compartments occurs by trans-endothelial permeability and lymphatic flow. Soluble species are degraded in the tissue or cleared from the blood. Specifically, the compartment model includes: (B) The molecular interactions of two active VEGF isoforms ($VEGF_{121}$ and $VEGF_{165}$), receptors (R1 and R2), and co-receptors (N1 and N2); (C) The interactions between TSP1, its receptors (CD36, CD47, β1, and LRP1), VEGF and VEGFR2; (D) The activation of proMMP9 via cleavage by MMP3; cleavage of TSP1; proteolysis of $VEGF_{165}$ (free or bound to glycosaminoglycan, GAG, chains) to form $VEGF_{114}$ by active MMPs; (E) The sequestration of $VEGF_{165}$ and TSP1 by GAG chains in the extracellular matrix and the cellular basement membranes; (F) The sequestration of VEGF by α2M in blood; (G) The binding between ABT-510 and receptors; sequestration of VEGF by bevacizumab.

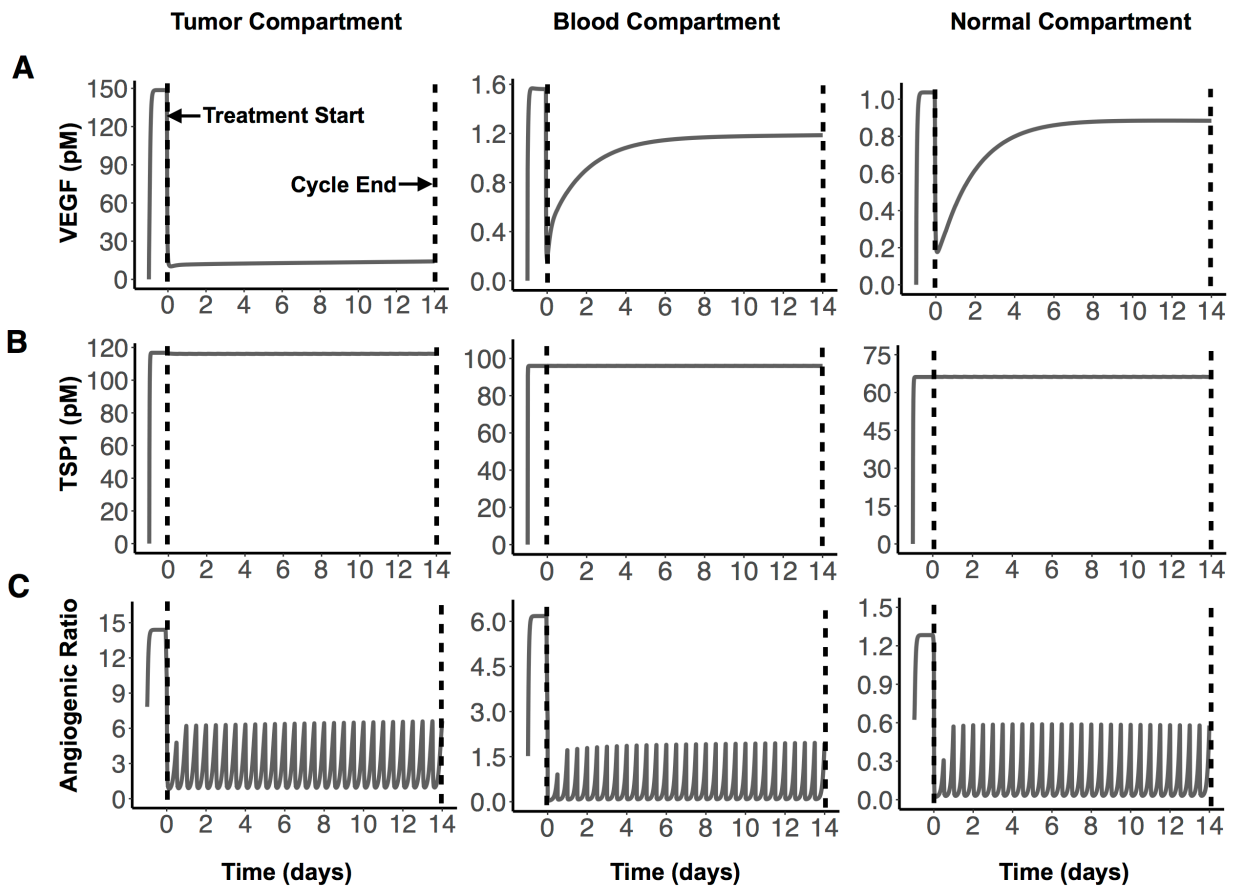

Figure 2. The effects of one cycle of combination anti-angiogenic therapy. The system is allowed to reach steady state before the start of treatment (Day 0). One cycle of treatment lasts 14 days: bevacizumab is given once every two weeks, and ABT-510 is given twice daily. (A) VEGF is shown to decrease after the treatment start in all three compartments. (B) TSP1 is predicted to stay at a stable level. (C) The angiogenic ratio (the ratio of pro-angiogenic complexes to anti-angiogenic complexes) is predicted to oscillate.

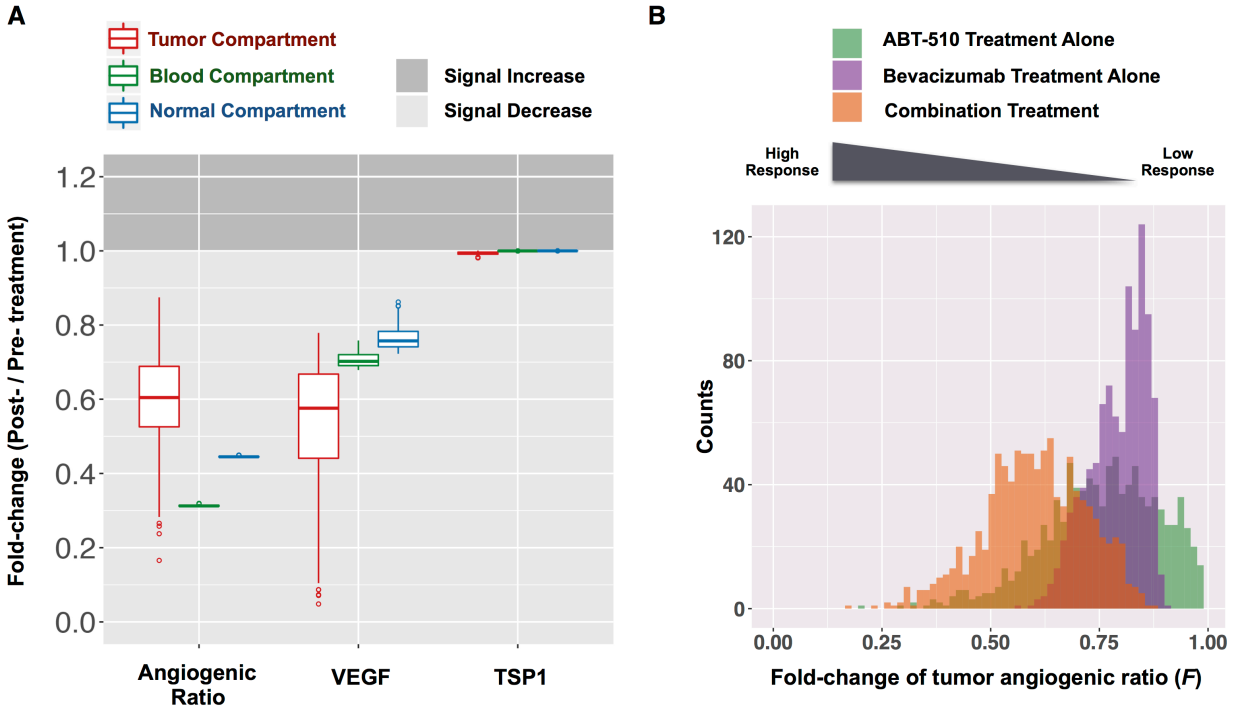

Figure 3. The impact of tumor receptor heterogeneity on the response to anti-angiogenic therapy. We simulated 1,000 tumor receptor profiles and predict: (A) The fold-changes of the angiogenic ratio, VEGF and TSP1 in tumor (red), blood (green) and normal (blue) compartments. (B) The distributions of the fold-change in the tumor angiogenic ratio (F) for single-agent treatments and combination therapy (green: ABT-510 alone; purple: Bevacizumab alone; orange: Combination treatment).

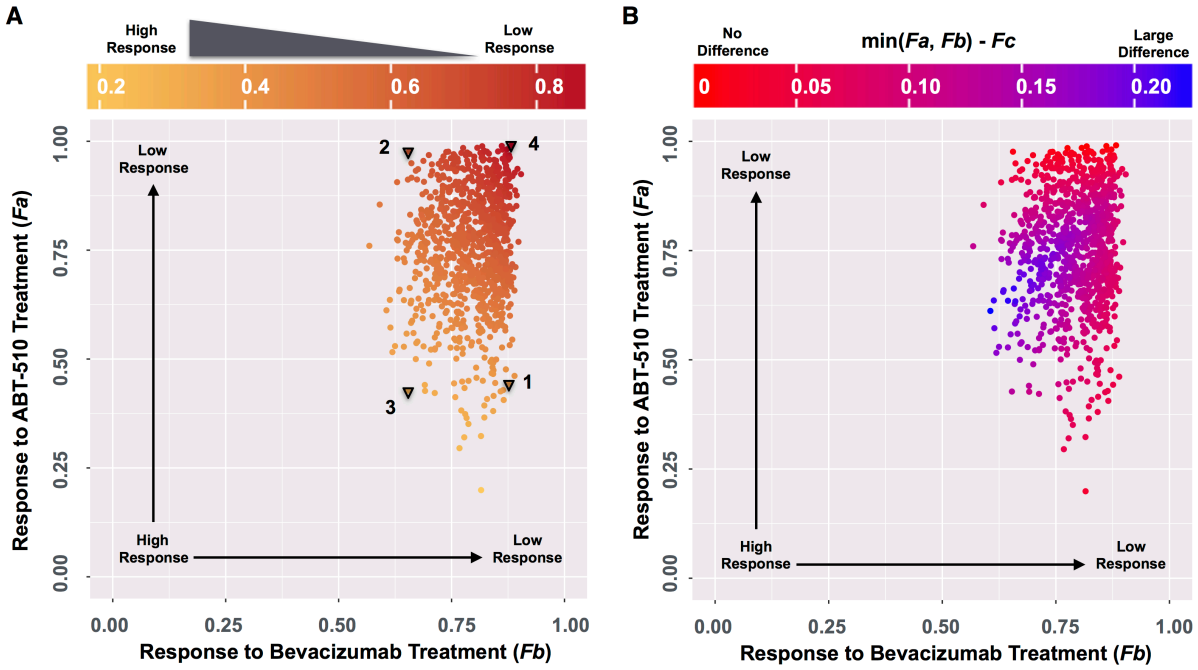

C

Patient	Fc	Dose A (mg/kg)	Dose B (mg)	Dose a (mg/kg)	Dose b (mg)	CI
2	0.64	12	3949	10	100	0.89
4	0.87	11	2228	10	100	0.97
3	0.29	95	183	10	100	0.65
1	0.39	193	124	10	100	0.89

Figure 4. The impact of tumor receptor heterogeneity on the combination effect. (A) The comparison of the response to combination therapy (Fc) and responses to single agent treatments (Fa: response to ABT-510 alone; Fb: response to bevacizumab alone). (B) The comparison of the response to combination therapy (Fc) and the best response between the individual treatments (the smaller of Fa and Fb). (C) The calculated Combination Index (CI) for four representative tumor receptor profiles.

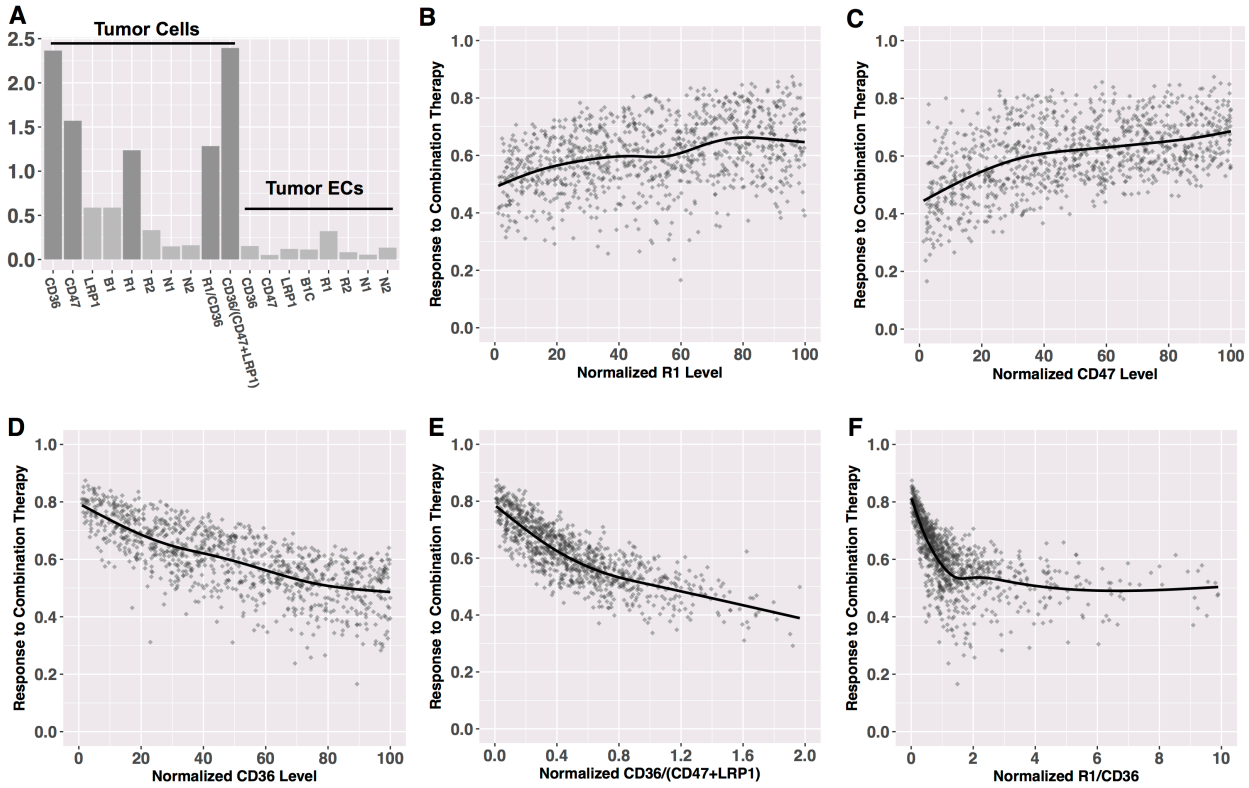

Figure 5. The association between tumor angiogenic receptors and the response to combination anti-angiogenic therapy. (A) The calculated variable importance of projection (VIP) score estimated for the PLSR model. VEGFR1, CD36 and CD47 on tumor cells have VIP scores higher than one (dark grey bars), indicating that they each significantly contribute to the response to treatment, the fold-change in the angiogenic ratio in the tumor. (B-F) The associations between normalized receptor level and the response to combination therapy. The black line is the locally weighted scatterplot smoothing (LOWESS).

Supplementary Data:

Supplementary File S1. This zipped file contains the computational model used to generate the results presented in this paper: “TSP1_VEGF_Model.m”, the MATLAB *m*-file containing the whole-body TSP1-VEGF model; “run_baselinedynamics.m”, “run_MCsimulations.m”, the MATLAB scripts to run the baseline model and Monte Carlo simulations, respectively; and “findParamValue_Rec.m” the MATLAB script to randomly generate the receptor number.

Supplementary File S2. Model parameters.

Supplementary File S3. Supplementary figures and captions.